UMP-91/08.
(OZ-91/03).

Bilocal Bosonization of QCD and Electroweak Properties of Light Pseudoscalar Mesons

C.I.Belyea and B.H.J.McKellar
Research Centre for High Energy Physics,
School of Physics,
University of Melbourne,
Parkville,
Vic 3052 AUSTRALIA.

QCD-based analysis of the low energy electroweak properties of light pseudoscalars is studied using an approximate bilocal bosonization technique. Particular attention is given to the problem of maintaining electroweak gauge invariance, and a bilocal Wilson-line technique is introduced to address this problem. The decay constants F_K and F_π and the $\pi^\pm$ charge radius are discussed in detail.

I. INTRODUCTION

Bilocal fields [1-14] have been used in recent years to address the difficult problem of extracting quantitative low-energy hadron properties from the fundamental QCD dynamics of quarks and gluons. A broad aim of this field is to bridge analytically the gulf which separates QCD from the low-energy phenomenological principles of the 1960's and provide detailed analysis of the spontaneous breaking of the (approximate) chiral symmetry. Simplified models such as Nambu-Jona-Lasinio four-Fermi interaction [17-19] (NJL) and cloudy bag model [20] exhibit some of the qualitative low-energy features of the strong interaction, but have only a loose connection with QCD. Analytical models based on systematic truncations of QCD can claim to be closer to the exact QCD dynamics than the models discussed above.

Such a model has been developed by Cahill, Roberts and Praschifka [6-14] using an auxiliary field approach to bilocal bosonization. They show how QCD may be formally transformed from the quark-gluon description into a nonlocal meson-diquark form and subsequently partially re-summed into a theory of mesons and baryons. With the aid of a simplifying truncation of QCD called the Global Color Model (GCM), they are able to discuss in detail the spontaneous breaking of chiral symmetry and the almost-Nambu-Goldstone (NG) bosons (π, K). Lowest order calculations indicate that PCAC results and GMOR mass relations [6,8,14,15] emerge naturally in the GCM.

It is this successful detailed treatment of the light NG bosons which we wish to exploit here to examine some electroweak properties of pions and kaons. The GCM is a non-local model, which complicates the calculation of electroweak effects compared with local NJL models. After reviewing the definition of the GCM in the next section, we will discuss two methods by which electroweak (EW) effects may be calculated: one EW gauge covariant but computationally difficult; the other computationally simpler but non-EW gauge covariant. Both methods will be employed to investigate in particular the decay constants F_π and F_K and the π charge radius.

II. BILOCAL BOSONIZATION AND THE GCM

Cahill, Roberts and Praschifka start with the generating functional of Euclidean QCD, which with quark sources $\eta, \bar{\eta}$ may be written[11-13]

$$Z[\eta,\bar{\eta}] = e^{W_1\left[ig\frac{\delta}{\delta\eta}\frac{\lambda^a\gamma_\mu}{2}\frac{\delta}{\delta\eta}\right]}\int D\bar{q}Dq e^{-S[q,\bar{q}]+\int \bar{q}\eta+\bar{\eta}q} \tag{1}$$

where

$$S[q,\bar{q}] = \int \bar{q}(\not{\partial}+m)q + \int d^4x d^4y \frac{g^2}{2} D^{ab}_{\mu\nu}(x-y;\xi)\bar{q}(x)\gamma_\mu\frac{\lambda^a}{2}q(x)\bar{q}(y)\gamma_\nu\frac{\lambda^b}{2}q(y) \tag{2}$$

and

$$W_1[J] = \sum_{n=3}^{\infty} \int d^4x_1 \ldots d^4x_n \frac{1}{n!} D^{a_1 \ldots a_n}_{\mu_1 \ldots \mu_n}(x_1 \ldots x_n; \xi) \prod_{i=1}^{n} J^{a_i}_{\mu_i}(x_i) \tag{3}$$

$D^{a_1 \ldots a_n}_{\mu_1 \ldots \mu_n}$ is the full (reducible) n-point function for pure QCD (without quarks), m is the quark current mass matrix and ξ is the gauge parameter.

If the gauge group were $U(1)$, $D_{\mu\nu}$ would be the free photon propagator and we would have $W_1 = 0$, since all the pure QED ($n > 2$)-point functions are zero. While $W_1 \neq 0$ for QCD as a result of gluon-gluon coupling, the truncation of (1) by setting $W_1 = 0$ (and consequently $S[q, \bar{q}]$ becoming the full action) is not as severe as neglecting all gluon-gluon interactions since such effects are already present in the confining pure QCD 2-point function $D^{ab}_{\mu\nu}$. Fig. 1 shows examples of three qq scattering diagrams which are part of the perturbation expansion of QCD. Fig. 1(c) is excluded by setting $W_1 = 0$, whereas 1(a) and 1(b) are still included. This can be compared with the 'quenched approximation' [22] popular in lattice QCD which would instead exclude all diagrams containing quark loops, such as 1(b). It would be controversial to claim that truncating to $W_1 = 0$ is a true approximation of QCD (valid to a known accuracy in well-defined physical circumstances), and such a truncation may be criticized on the basis that the local $SU(3)$ color symmetry is reduced to global $SU(3)$. However, at the very least $S[q, \bar{q}]$ is an interesting cousin of QCD which retains many of the important properties of the full gauge-invariant theory: dynamical quarks, global color, confinement (at least for mesons), Lorentz invariance (or $SO(4)$ invariance in Euclidean space) and chiral symmetry in the limit $m \to 0$. We will henceforth refer to the system whose full action is given by S as the Global Color Model (GCM). For the sake of completeness we present here a summary of the steps by which Cahill et.al. transform the GCM into a nonlocal theory of mesons and diquarks.

Since the form of the full pure QCD 2-point function is known only at high energies, which is insufficient for low-energy hadron properties, Cahill et.al. use the ansatz

$$g^2 D^{ab}_{\mu\nu}(x - y) = \delta_{\mu\nu}\delta^{ab} D(x - y); D(x - y) = \int \frac{d^4q}{(2\pi)^4} \frac{\alpha(q^2)}{q^2} e^{iq\cdot(x-y)} \tag{4}$$

containing in the functional form of the running coupling $\alpha(q^2)$ both strong peaking at low q^2 due to confinement and at high q^2 the standard logarithmic form derived from the renormalization group equations[11]. The Euclidean GCM action may now be written

$$\begin{aligned} S = & \int \bar{q}(\not{\partial} + m)q \\ & + \frac{1}{2} \int_{xy} D(x - y)\bar{q}(x)\gamma_\mu \frac{\lambda^a}{2} q(x)\bar{q}(y)\gamma_\mu \frac{\lambda^a}{2} q(y) \end{aligned} \tag{5}$$

The bilocal four quark term is then manipulated into a form containing bilocal arrangements appropriate for mesons ($\bar{q}(x)Mq(y)$) and diquarks ($q^T(x)Mq(y)$) by means of the following Fierz transformations:

Dirac:

$$(\gamma_\mu)_{rs}(\gamma_\mu)_{tu} = K^a_{ru}K^a_{ts} = (K^aC^T)_{rt}(C^TK^a)_{us}$$

where $\{K^a\} = \{1, i\gamma_5, \frac{i}{\sqrt{2}}\gamma_\mu, \frac{i}{\sqrt{2}}\gamma_\mu\gamma_5\}$

and C is the charge conjugation matrix

Color:

$$(\lambda^a)_{\alpha\beta}(\lambda^a)_{\gamma\delta} = \frac{4}{3}\delta_{\alpha\delta}\delta_{\beta\gamma} - \frac{2}{3}\epsilon_{\rho\alpha\gamma}\epsilon_{\rho\beta\delta}$$

Flavor:

$$\delta_{ij}\delta_{kl} = F^c_{il}F^c_{kj} = F^c_{ik}F^c_{lj}$$

where $\{F^c\} = \{\frac{1}{\sqrt{2}}1, \frac{1}{\sqrt{2}}\tau_i\}$ or $\{\frac{1}{\sqrt{3}}1, \frac{1}{\sqrt{2}}\lambda^a\}$

for 2 or 3 flavors (6)

This Fierz transformation is unique if one requires the non-existence of objects sucl as color octet mesons or color sextet diquarks which are believed not to be dynamically favoured. The transformed action is then

$$\begin{aligned} S[\bar{q},q] = &\int \bar{q}(\not{\partial} + m)q \\ &- \int_{xy} \frac{1}{8}\bar{q}(x)M^\theta_m q(y)D(x-y)\bar{q}(y)M^\theta_m q(x) \\ &- \int_{xy} \frac{1}{8}\bar{q}(x)M^\phi_d C^T\bar{q}^T(y)D(x-y)q^T(y)C^TM^\theta_m q(x) \end{aligned} \quad (7)$$

where $M^\theta_m = \frac{2}{\sqrt{3}}K^AF^C$ and $M^\phi_d = \sqrt{\frac{2}{3}}K^A\epsilon_\rho F^C$.

The quartic quark terms are then converted into quadratic form by introducing bilocal fields $\mathcal{B}^\theta(x,y)$, $\mathcal{D}^\phi(x,y)$ and $\bar{\mathcal{D}}^\phi(x,y)$. For example, the meson-channel identity is

$$\begin{aligned} &exp\ \Big\{ - \int_{xy} \frac{1}{8}\bar{q}(x)M^\theta_m q(y)D(x-y)\bar{q}(y)M^\theta_m q(x)\Big\} \\ &\quad = A\int D\mathcal{B} exp\Big\{ - \int_{xy} \frac{1}{2D(x-y)}\mathcal{B}^\theta(x,y)\mathcal{B}^\theta(y.x) + \bar{q}(x)\frac{M^\theta_m}{2}q(y)\mathcal{B}^\theta(x,y)\Big\} \end{aligned} \quad (8)$$

A is an unimportant constant and the meson bilocal field is defined to be Hermitian ($\mathcal{B}^\theta(x,y)^* = \mathcal{B}^\theta(y,x)$) since the anti-Hermitian part is non-interacting. The quarks may now be integrated out and the system expressed as a path integral over $\mathcal{B}$, $\mathcal{D}$ and $\bar{\mathcal{D}}$. The action is then expanded about a stationary point obeying

$$\frac{\delta S}{\delta \mathcal{B}} = \frac{\delta S}{\delta \mathcal{D}} = \frac{\delta S}{\delta \bar{\mathcal{D}}} = 0. \tag{9}$$

The non-trivial stationary point is assumed to be dynamically preferred to the trivial one $\mathcal{B} = \mathcal{D} = \bar{\mathcal{D}} = 0$ since the former spontaneously breaks chiral symmetry in the chiral limit. The non-trivial solution is parametrized by

$$\begin{aligned} G^{-1}(x,y) &= (\not{\partial} + m)_{xy} + \frac{1}{2} M^{\theta}_{m} \mathcal{B}^{\theta}_{cl}(x-y) = \int \bar{d}^4 q e^{iq\cdot(x-y)} G^{-1}(q) \\ \text{where } G^{-1}(q) &= i \not{q} A(q^2) + m + B(q^2) \\ \mathcal{D}^{\phi}_{cl} &= \bar{\mathcal{D}}^{\phi}_{cl} = 0 \end{aligned} \tag{10}$$

$A(q^2)$ and $B(q^2)$ (plotted in Fig. 2) are independent of m for small m and will be further discussed below.

The quantum fluctuations of $\mathcal{B}$ and $\mathcal{D}$ are interpreted as mesons and diquarks. Since in this paper we are interested only in the pseudoscalar NG bosons, we will assume that the diquark fluctuations may be ignored and set $\mathcal{D} = \bar{\mathcal{D}} = 0$. The meson action may then be written, after performing the redefinition $\mathcal{B} \to \mathcal{B} + \mathcal{B}_{cl}$

$$\begin{aligned} S[\mathcal{B}] = &-Tr\ ln\ (G^{-1} + \frac{1}{2} M^{\theta}_{m} \mathcal{B}^{\theta}) \\ &+ \int_{xy} \frac{1}{2D(x-y)} (\mathcal{B}^{\theta} + \mathcal{B}^{\theta}_{cl})_{xy} (\mathcal{B}^{\theta} + \mathcal{B}^{\theta}_{cl})_{yx} \end{aligned} \tag{11}$$

The full trace over spacetime and internal indices is denoted Tr. That G plays the role of a nonperturbative quark propagator may be seen by reconverting the $Tr\ ln$ with effective quark fields Q via

$$exp\ [Tr\ ln(G^{-1} + \frac{1}{2} M^{\theta}_{m} \mathcal{B}^{\theta})] = \int D\bar{Q} D Q exp\ [-\bar{Q}(G^{-1} + \frac{1}{2} M^{\theta}_{m} \mathcal{B}^{\theta}) Q] \tag{12}$$

in an obvious matrix notation. It is a consequence of expanding $\mathcal{B}^{\theta}$ about the stationary point that terms linear in $\mathcal{B}^{\theta}$ (tadpoles) arising from the expansion of the $Tr\ Ln$ are exactly cancelled by the linear part of the second term in equation (11).

With the use of a complete set of structure functions Γ^{θ}_{A} the bilocal field may then be expressed in terms of local fields ϕ^{θ}_{A} carrying meson quantum numbers :

$$\mathcal{B}^{\theta}(x,y) = \sum_{A=1}^{\infty} \Gamma^{\theta}_{A}(x-y, \frac{x+y}{2}) \phi^{\theta}_{A}(\frac{x+y}{2}) \tag{13}$$

The Γ^{θ}_{A} are fixed by requiring diagonalization of the induced kinetic and mass terms for the ϕ^{θ}_{A} contained within S. In momentum space

$$S_{\phi^\theta_A \phi^{\theta'}_{A'}} = \delta^{\theta\theta'}\delta_{AA'} \int \bar{d}^4 p \phi^\theta_A(p)\phi^\theta_A(-p)\lambda^\theta_A(p^2) \tag{14}$$

The eigenvalues of the diagonalization are $\lambda^\theta_A(p^2)$. On mass shell this process is equivalent to solving the Bethe-Salpeter equation for the bound state structure functions Γ in the ladder approximation [21] The meson mass $\mathcal{M}$ is given by the zeros (if any) of $\lambda(-\mathcal{M}^2) = 0$, since if λ has such a zero we may then write

$$\lambda(p^2) = f(p^2)^2(p^2 + \mathcal{M}^2) \tag{15}$$

In our analysis we will absorb the normalization constant f by a momentum dependent rescaling of the meson field

$$\phi(p) \rightarrow \phi(p) f(p^2) \tag{16}$$

which not only furnishes the fields ϕ with the appropriate dimensionality but also produces a point-like kinetic term so that all the effects of compositeness are manifest in the interaction vertices.

For the NG family, (for which $M^\theta_m \sim i\gamma_5 \tau^I$) the diagonalization in the chiral limit yields $\mathcal{M} = 0$ and

$$\Gamma_\pi = \Gamma_\pi(x - y) = \int \bar{d}^4 q e^{iq\cdot(x-y)} B(q^2) \tag{17}$$

on the mass shell $p^2 = 0$ with $B(q^2)$ defined in (10). The kinetic and mass terms involved in the diagonalization are schematically illustrated in Fig. 3. 3(a) comes from the second term of (11) and being a contact term contributes only to the mass. The quark propagator is drawn in this diagram since

$$\frac{1}{2D(x-y)} = tr\ G(x,y) \tag{18}$$

where tr is a trace over internal indices only. Fig. 3(b) is the quadratic term in the expansion of the $Tr\ ln$ via

$$Tr\ ln\ (a^{-1} + x) = Tr\ ln\ a^{-1} + Tr\ (ax) - \frac{1}{2} Tr\ (axax) + \ldots \tag{19}$$

and contributes both mass and kinetic terms. The massless NG character of the pseudoscalar family emerges from an exact cancellation between the mass contributions from Figs. 3(a) and 3(b), the cancellation depending on the result (17).

By assuming that the quark current mass m constitutes a small perturbation about the chiral limit, and that (17) holds away from $p^2 = 0$, Cahill et.al. reproduce [6] the PCAC formula

$$\mathcal{M}_\pi^2 = \frac{\hat{m}}{f_\pi^2}\langle\bar{q}q\rangle \tag{20}$$

where $\hat{m}$ is an $SU(3)$-based current mass average for the particular meson. The $GMOR$ mass relations also emerge [15].

Although a full treatment of the NG bosons would involve finding explicitly the full form of $\Gamma_\pi(p,q)$, in the absence of such an effort we will also assume in this paper that

$$\Gamma_\pi(p,q) = B(q^2) \text{ up to } p^2 = -\mathcal{M}_K^2 \tag{21}$$

and hence for θ such that $M_m^\theta \sim i\gamma_5\tau^I$ make the following substitution in equation (11):

$$\frac{1}{2}M_m^\theta B^\theta(x,y) = i\gamma_5\tau^I B(x-y)\pi^I(\frac{x+y}{2}) \tag{22}$$

Consistent with (22) is the assumption that the form of $f_\pi(p^2)$ may be obtained by computing the p^2 behaviour of Fig. 3(b).

In ref. [14] an alternative definition was made for the NG bosons using the expansion

$$\frac{1}{2}M_m^\theta B^\theta = B(x-y)[\exp\left\{i\gamma_5\pi^I(x)\tau^I\right\} - 1] \tag{23}$$

which keeps the chiral symmetry manifest and leads to an effective non-linear chiral lagrangian in terms of the field $\exp\left\{i\pi^I(x)\tau^I\right\}$ at low energies. However since we will not be concerning ourselves here with EW processes involving more than two NG bosons, our results are easier to obtain with the use of the simpler substitution (22). In the processes we consider the low energy electroweak properties of the pion will follow exactly the predictions of chiral symmetry. The use of (23) enabling direct connection with the phenomenology of chiral perturbation theory would be an interesting subject of further study.

In this paper we will consider only tree level process in the meson sector. The composite meson propagators given by (14) of course suffer corrections in the effective action (obtained by introducing meson and diquark sources and performing a Legendre transformation) due to meson and diquark loops. Examples of such corrections to the effective meson propagator $\langle\phi_A^\theta(\frac{x+y}{2})\phi_{A'}^{\theta'}(\frac{z+w}{2})\rangle$ are shown in Fig. 4. The loop corrections affect the effective theory not only by necessitating a renormalization of the fields ϕ, but also by introducing both off-diagonal elements in the propagator and ϕ tadpoles, shown in Fig. 5. The off-diagonal corrections reflect the difference between the ladder approximation to the Bethe-Salpeter structure functions and the full effective $\langle\bar{Q}Q\phi\rangle$ vertex, and the tadpoles reflect the inexact nature of the ladder approximation vacuum characterised by $B_{cl}^\theta(x-y)$. Since the structure

functions Γ provide short-distance cutoffs at the compositeness scale, these effects are finite but may constitute a substantial correction to the tree level results. This is a long-standing problem with low-energy phenomenological actions and in this model accurate estimation of such corrections is a formidable task, requiring even at one loop level a complete knowledge of the meson and diquark (ladder approximation) structure functions.

A and B satisfy integral equations which are related to the Schwinger-Dyson equation for the quark propagator G in the ladder approximation [2,6]. A careful analysis shows however that the equations differ from the ladder approximation by a factor which varies depending on the particular color Fierz transformation used[21], a difference which only concerns effects in the diquark sector at tree level. This phenomenon has recently been resolved by Lutz and Praschifka[23].

In this paper we use the numerical solution for A and B[11,12], plotted in Fig. 2. These solutions were scaled essentially so as to produce the correct chiral-invariant mass which is the dominant contibution to all hadrons except the NG bosons. The functions A and B are obtained from the stationary solutions of a Euclidean action, and we make the standard assumption that the effective meson actions which we derive from the theory may be rotated back into Minkowski space. In the current context, singularities have been shown to exist in the effective Euclidean quark propagator which might prevent the Wick rotation of the effective meson theory. [16] This is a situation which also arises in similar analyses of QED [24]. The issue of whether or not the Wick rotation can be justified in a non-perturbative analysis is in general unresolved and also of course affects the validity of lattice computations.

III. INCLUSION OF ELECTROWEAK EFFECTS

A. Formalism

The inclusion of electroweak fields, generically labelled H_μ, modifies (5) at low energies to

$$S[q,\bar{q},H] = \int \bar{q}(\partial\!\!\!/ + m + ig_H H\!\!\!/_L)q + \frac{1}{2}\int_{xy} D(x-y)\bar{q}(x)\gamma_\mu\frac{\lambda^a}{2}q(x)\bar{q}(y)\gamma_\mu\frac{\lambda^a}{2}q(y) + S_{kin}[H]\,, \qquad (24)$$

where H_μ is in general a flavor matrix and the subscript 'L' indicates a left-handed projection operator $P_L = \frac{1}{2}(1-\gamma_5)$ where appropriate. Since we are only interested in effects well below the energy level of EW spontaneous symmetry breaking, in the case of the weak interactions the W-boson 'kinetic' term is approximated by

$$S_{kin}[W] = \int m_W^2 W_\mu^+ W_\mu^- \qquad (25)$$

which immediately integrates in the path integral to produce the Fermi current-current interaction. Rather than use the equivalent Fermi form, we present the low energy theory with the use of the $W_\mu^\pm$ (or equivalently the isovector W_μ^I) since the gauge-invariant interaction term helps to clarify the discussion of current conservation issues in the following sections.

B. Bare vertex method

The most straightforward way to carry out the bosonization procedure in the presence of H_μ is to simply perform the identical steps already described for $H_\mu = 0$. Explicitly, we perform the same Fierz transformation as given in (6) and expand about

$$\frac{\delta S}{\delta \mathcal{B}} = 0 \quad \text{at } H_\mu = 0 \tag{26}$$

which yields after integrating out the quarks

$$\begin{aligned} S[\mathcal{B}, H] = &-Tr\ ln(G^{-1} + ig_H\ \not{H}_L + \frac{1}{2}M_m^\theta \mathcal{B}^\theta) \\ &+ \int_{xy} \frac{1}{2D(x-y)}(\mathcal{B}^\theta + \mathcal{B}_{cl}^\theta)_{xy}(\mathcal{B}^\theta + \mathcal{B}_{cl}^\theta)_{yx} + S_{kin}[H] \end{aligned} \tag{27}$$

Expansion of the $Tr\ ln$ produces EW interactions with the mesons ϕ where the $H\bar{Q}Q$ vertex is given by its bare value. Momentum space details of diagrams relevant to $\pi^\pm$ charge and charge radius, $\pi^\pm$ decay constant and anomalous $\pi^0 \to \gamma\gamma$ decay are shown in Fig. 6. Use of the bare vertices (in different models) has been considered recently by McKay and Munczek [4] and also Gogokhiac et. al[5].

Ideally one would like the tree-level interaction terms to reflect known symmetry-dependent low-energy properties, in particular

- the charge of the $\pi^\pm$ is exactly $\pm e$;
- in the chiral limit $F_\pi = f_\pi$, where F_π is the pion decay constant and f_π is the normalization constant of the pion field, as predicted by the gauged nonlinear σ-model;
- in the chiral limit the $\pi^0\gamma\gamma$ term has the form and strength predicted by chiral symmetry quantum consistency arguments [28].

At lowest order in the EW coupling strength g_H, all these properties are essentially a result of the global symmetries $SU(N)_A \otimes SU(N)_V \otimes U(1)_V$ which give rise to electromagnetic and weak current conservation, and will only remain manifest at tree

level if the $\bar{Q}QH_\mu$ vertices in Fig. 6 obey the appropriate Ward Identities. The bare vertices fail this test as a result of the momentum dependence of the functions $A(q^2)$ and $B(q^2)$ appearing in the nonperturbative effective quark propagator $G(q)$. For example, to guarantee the correct pion charge from diagram 6(b) would require the replacement of γ_μ with a vertex $V_\mu(q,k)$ such that

$$V_\mu(q,0) = -i\partial_\mu G^{-1}(q) \tag{28}$$

where k_μ is the momentum carried by the photon. Such a problem does not appear in constituent quark models or the point-like Nambu-Jona-Lasinio models which use effective quark propagators of the form $1/(i\not{q}+M)$ with M the (constant) constituent mass.

While the bare vertex method is thus flawed in failing the Ward identities at each order in the 'meson loop' expansion, it has the advantage of computational simplicity and moreover it is important to find out the size of the discrepancy which it produces in the relevant processes. Before developing an improved bosonization, we provide in what follows the ultra-low energy limit of the processes shown in Fig. 6.

1. $\pi - W$ interaction

In position-space the $\pi - W$ coupling is given by

$$S_{\pi W} = \cos\theta_c \; tr \int_{xyz} \pi^I(\frac{x+y}{2}) i\gamma_5 \tau^I B^R_{yz} G_{xz} i\frac{g'}{2}\gamma_\mu P_L \tau^J W^J_\mu(z) G_{zy} \tag{29}$$

where θ_c is the Cabbibo angle and we have used an index notation for compactness. The momentum space form is (Fig. 6(a))

$$\begin{aligned} S_{\pi W} = \cos\theta_c \int d^4p d^4q \pi^I(p) W^J_\mu(-p) \\ tr\ \{i\gamma_5\tau^I \frac{B(q^2)}{f_\pi(p^2)} G(q-\tfrac{1}{2}p) i\frac{g'}{2}\gamma_\mu P_L \tau^J G(q+\tfrac{1}{2}p)\} \end{aligned} \tag{30}$$

In (29). $B^R(x,y)$ is the position space equivalent of the rescaled pion structure function $B(q^2)/f_\pi(p^2)$ in momentum space.

To lowest order in p_μ this reduces to

$$\begin{aligned} S_{\pi W} &= -\cos\theta_c \frac{g'}{2}\frac{I_{\pi W}}{f_\pi(0)} \int d^4p \; ip_\mu \pi^I(p) W^I_\mu(-p) \\ &= -\cos\theta_c \frac{g'}{2}\frac{I_{\pi W}}{f_\pi(0)} \int d^4x \partial_\mu \pi^I W^I_\mu \end{aligned} \tag{31}$$

where

$$I_{\pi W} = \frac{1}{16\pi^2}\int_0^\infty ds\; sB(s)[2s(X'Y - XY') + 4XY] \tag{32}$$

X and Y are defined in terms of A and B via $G(q) \equiv -i\not{q}X(q^2) + Y(q^2)$.

The pion normalization is obtained from the process shown in Fig. 3 which gives

$$S_{\pi\pi} = \tfrac{1}{2}\int d^4p d^4q tr\{ i\gamma_5\tau^I\pi^I(-p)B(q^2)G(q-\tfrac{1}{2}p) \\ i\gamma_5\tau^J\pi^J(p)B(q^2)G(q+\tfrac{1}{2}p)\} + \Delta_m \tag{33}$$

where Δ_m is the cancelling mass contribution from Fig. 3(a). Taking the low p^2 limit, $f_\pi(0) \equiv f_\pi$ is given by

$$f_\pi^2 = \frac{6}{16\pi^2}\int_0^\infty ds\; sB^2(s)[X^2 + s^2X'^2 + sY'^2 \\ -2sXX' - s^2XX'' - 2YY' - sYY''] \tag{34}$$

with the chiral limit result $f_\pi = 70$ MeV. It is not the comparison of f_π or F_π with the experimental value of 93 Mev which is important to the current discussion, rather the desired relation

$$F_\pi \equiv I_{\pi W}/f_\pi = f_\pi\ . \tag{35}$$

The formula (32) gives $F_\pi = 0.49 f_\pi$. Thus in this case the bare vertex method gives a large discrepancy at zeroth order. It will be shown later that the discrepancy of a factor of approximately 2 is related to the fact that $A(q^2)$ is slowly varying and approximately equal to 2 at low q^2.

2. $\pi\pi\gamma$ interaction

Fig. 6(b) yields

$$S_{\pi\pi A} = -\int d^4p d^4k d^4q \\ tr\{ i\gamma_5\pi^I(p)\tau^I\frac{B(q^2)}{f_\pi(p^2)}G(q-\tfrac{1}{2}p)i\gamma_5\pi^J(-p-k)\tau^J \\ \times\frac{B((q+\frac{1}{2}k)^2)}{f_\pi(p^2)}G(q+\tfrac{1}{2}p+k)ieQ\gamma_\mu A_\mu(k)G(q+\tfrac{1}{2}p)\} \tag{36}$$

$Q = \begin{pmatrix} -\frac{1}{3} & 0 \\ 0 & \frac{1}{3}\end{pmatrix}$ is the quark charge matrix

To lowest order in p and k this reduces to

$$S_{\pi\pi A} = Ke\int d^4p d^4k\; ip_\mu\epsilon^{IJ3}\pi^I(p)\pi^J(-p-k)A_\mu(k) \\ = -iKe\int A_\mu(\partial_\mu\pi\pi^* - \partial_\mu\pi^*\pi) \tag{37}$$

where $\pi \equiv (\pi^1 - i\pi^2)/\sqrt{2}$ and

$$K = \frac{3}{16\pi^2 f_\pi^2}\int_0^\infty dsdB^2X(3sX^2 + Y^2) \tag{38}$$

$K = 0.78$ instead of the integral-charge value 1. If we use instead of the bare vertex the Ward-Identity-preserving vertex

$$iQ\gamma_\mu \to Q\partial_\mu G^{-1}(q) \tag{39}$$

then (37) becomes at $k = 0$

$$S_{\pi\pi A} = i\frac{3e}{f_\pi^2}\int \bar{(d)}^4 p\bar{d}^4k\ \epsilon^{IJ3}\pi^I(p)\pi^J(-p-k)A^\mu(k)T_\mu(p,0) \tag{40}$$

where, using $G\partial_\mu G^{-1}G = -\partial_\mu G$,

$$\begin{aligned} T_\mu(p,0) &= i\int \bar{d}^4 qB(q^2)^2 tr^D\{\gamma_5 G(q-\tfrac{1}{2}p)\gamma_5\partial_\mu G(q+\tfrac{1}{2}p)\} \\ &= i\frac{\partial}{\partial p_\mu}\int \bar{d}^4 qB(q^2)^2 tr^D\{\gamma_5 G(q-\tfrac{1}{2}p)\gamma_5 G(q+\tfrac{1}{2}p)\} \\ &= \frac{i}{3}\frac{\partial}{\partial p_\mu}\left[\tfrac{1}{2}p^2 f_\pi^2 + \mathcal{O}(p^4)\right]\ .\} \end{aligned} \tag{41}$$

The f_π^2 factors cancel and $K = 1$ results. In the next section a gauge covariant bosonization will be developed which produces both this result and $F_\pi = f_\pi$.

3. $\pi\gamma\gamma$ interaction

As shown in Fig. 6(c) this interaction, which is responsible for the anomalous $\pi^0 \to \gamma\gamma$ decay is given by

$$\begin{aligned} S_{\pi AA} = -\int \bar{d}^4 l\bar{d}^4 m\bar{d}^4 q\ tr\{&G(q-\tfrac{1}{2}l)i\gamma_5\tau^I\pi^I(-l-m)\frac{B(q^2)}{f_\pi(p^2)} \\ &G(q+\tfrac{1}{2}m+\tfrac{1}{2}l)ieQ\gamma_\mu A_\mu(m)G(q-\tfrac{1}{2}m+\tfrac{1}{2}l)ieQ\gamma_\nu A_\nu(l)\}\ . \end{aligned} \tag{42}$$

This reduces in lowest order of l and m to

$$\begin{aligned} &S_{\pi AA} \approx ie^2\frac{I_{\pi AA}}{f_\pi}\int d^4x\pi^0 F\tilde{F} \\ &\text{where } \pi^0 \equiv \pi^3\ ;\ \tilde{F}_{\mu\nu} \equiv \epsilon_{\mu\nu\alpha\beta}F_{\alpha\beta} \\ &\text{and } I_{\pi AA} = \int_0^\infty dsdB(s)(YX^2 + sY^2X' - sY'X^2) \end{aligned} \tag{43}$$

with the value $I = 0.068$. Wess and Zumino have argued that $I = 1/6 \approx 0.17$ (agreeing well with experiment) on the basis $S_{\pi AA}$ must be part of a gauged anomalous

Wess-Zumino (WZ) term [28]. In the absence of EW fields, the WZ term with the appropriate strength has also been shown to emerge from either parametrization (22) or (23) in the GCM [8,14]. The discrepancy using the bare vertex method may be approximately understood in terms of an accumulation of the charge discrepancy for the photon vertices:

$$0.068 \times \left(\frac{1}{0.78}\right)^2 = 0.11 \ . \tag{44}$$

C. Wilson line method

1. Formalism

Given the level of the charge-type discrepancies which appear in the zeroth order terms of the bare vertex method, it is important to indicate how the bosonization procedure may be modified so as to achieve exact low-energy results at tree level. As already discussed, the problem is essentially that Ward Identities connected with chiral and electromagnetic current conservation are not preserved at each order in the meson loop expansion, which can further be traced to the inappropriate EW gauge transformation properties of nonlocal structures such as $\bar{q}(x)M_m^\theta q(y)$ which are used in the bosonization. Such structures may be cured by joining the two points x and y by a Wilson line. This has previously been considered in the context of Bag models [25].

We introduce a Wilson line in the original GCM action (5) before the Fierz transformation is performed. First note that the following identity holds:

$$\begin{aligned} \bar{q}(x)\frac{\lambda^a}{2}\gamma_\mu q(x) &= \bar{q}_\Gamma(x;P)\frac{\lambda^a}{2}\gamma_\mu q_\Gamma(x;P) \\ \text{where } q_\Gamma(x;P) &= \mathcal{P}\exp\{i\int_{\Gamma[P,x]} g_H H_L \cdot ds\}q(x) \\ \text{and } \bar{q}_\Gamma(x;P) &= \bar{q}(x)\mathcal{P}\exp\{i\int_{\Gamma[x,P]} g_H H_R \cdot ds\} \end{aligned} \tag{45}$$

$\Gamma[x,P]$ denotes an arbitrary path from x to P, $\Gamma[P,x]$ denotes the same path from P to x, and $\mathcal{P}$ denotes path ordering. If P is a smooth function of x and y such that

$$P - P(x,y) = P(y,x) \ ; \ \ P(x,x) = x \tag{46}$$

then the first term of (24) can also be expressed in terms of the q_Γ as

$$\int \bar{q}(\partial\!\!\!/ + m + ig_H A\!\!\!/_L)q = \int_{xy} \bar{q}_\Gamma(x;P(x,y))(\partial\!\!\!/ + m)_{xy} q_\Gamma(y;P(x,y)) \ . \tag{47}$$

The Fierz transformation on the internal indices may then be performed as before, the Wilson lines becoming cross-linked as shown in Fig. 7. After bosonization,

$$S[\mathcal{B}] = -Tr\ ln\ M + \int_{xy} \frac{1}{2D(x-y)} (\mathcal{B}^\theta + \mathcal{B}^\theta_{cl})_{xy} (\mathcal{B}^\theta + \mathcal{B}^\theta_{cl})_{yx} \tag{48}$$

where

$$M_{xy} = \mathcal{P} \exp\{i \int_{\Gamma[x,P(x,y)]} g_H H_R \cdot ds\} \left\{G^{-1} + \tfrac{1}{2} M^\theta_m \mathcal{B}^\theta\right\} \mathcal{P} \exp\{i \int_{\Gamma[P(x,y),y]} g_H H_L \cdot ds\} \tag{49}$$

and the diquarks $\mathcal{D}, \bar{\mathcal{D}}$ have again been omitted. To first order in g_H,

$$\begin{aligned} M_{xy} = {} & G^{-1}_{xy} + \tfrac{1}{2} M^\theta_m \mathcal{B}^\theta_{xy} \\ & + i g_H \left\{ \int_{\Gamma[x,P(x,y)]} g_H H_R \cdot ds G^{-1}_{xy} + G^{-1}_{xy} \int_{\Gamma[P(x,y),y]} g_H H_L \cdot ds \right\} \\ & + i g_H \left\{ \int_{\Gamma[x,P(x,y)]} g_H H_R \cdot ds \tfrac{1}{2} M^\theta_m \mathcal{B}^\theta_{xy} + \tfrac{1}{2} M^\theta_m \mathcal{B}^\theta_{xy} \int_{\Gamma[P(x,y),y]} g_H H_L \cdot ds \right\} \end{aligned} \tag{50}$$

The different terms in M contibute respectively to $\phi\bar{Q}Q$, $H\bar{Q}Q$ and $\phi H\bar{Q}Q$ vertices in the expansion of $-Tr\ ln[1 + (GM - 1)]$. For the NG bosons, the local field substitution (22) is again employed.

In order to generate local interactions with the meson fields $\phi(\frac{x+y}{2})$ we choose the point P to be the midpoint: $P(x,y) = \frac{x+y}{2}$. Expanding the line integrals about P,

$$\begin{aligned} \int_{\Gamma[P,y]} H_\mu ds_\mu = {} & \tfrac{1}{2}(y-x)_\mu H_\mu(\frac{x+y}{2}) + c_1 (y-x)_\mu (y-x)_\nu \partial_\nu H_\mu(\frac{x+y}{2}) \\ & + c_2 (y-x)_\mu (y-x)_\nu (y-x)_\alpha \partial_\alpha \partial_\nu H_\mu(\frac{x+y}{2}) + \ldots \end{aligned} \tag{51}$$

and for the reverse path $\Gamma[x,P]$ the coefficients c_i are replaced by $(-1)^i c_i$. The c_i depend on the trajectory of the path Γ and for a straight line the first three are

$$c_1 = \frac{1}{8};\ c_2 = \frac{1}{48};\ c_3 = \frac{1}{384}\ . \tag{52}$$

In momentum space the $(y-x)_\mu$ terms become internal loop momentum derivatives $-i\partial/\partial q_\mu$ and $\partial_\nu H_\mu(\frac{x+y}{2})$ becomes $ip_\nu H_\mu(-p)$

An understanding of the Wilson line approach may be gained by examining the form of the term in M_{xy} which is linearly dependent only on H_μ. For the case of electromagnetism, and for zero photon momentum k_μ this term becomes $ieQ\partial_\mu G^{-1}(q)$

independently of the Wilson line trajectory. This form is the $k_\mu = 0$ solution to the Schwinger-Dyson equation for the photon vertex in the ladder approximation. At non-zero k_μ, a k_μ dependence will appear in this term which is dependent on the Wilson line trajectory. Using a straight Wilson line chooses a particular k_μ dependence which we assume is roughly similar to the ladder approximation vertex for non-zero k_μ. This choice may be viewed as the classical approximation of straight-line effective-quark propagation within the interaction vertex. Dependence of the physics on the Wilson line trajectory would only be expected to diasappear in the exact limit, when all orders in the loop expansion have been considered.

2. $\pi - W$ interaction

Defining $N \equiv (GM - 1)$, in the expansion of $-Tr\ ln(1 + N)$ both the $-Tr\ N$ and $\frac{1}{2}Tr\ N^2$ terms contribute to the low energy form $\int \partial_\mu \pi^I W^I_\mu$, as depicted in Fig. 8. Each term is dependent on the Wilson line trajectory (i.e. c_i-dependent) but the $-Tr\ N$ term exactly cancels the trajectory-dependence of the $\frac{1}{2}Tr\ N^2$ term thanks to the NG character of the pion expressed in the structure function relation $\Gamma_\pi = B$. This result is analogous to the cancellation between the two diagrams in Fig. 3 which leads to a massless pion in the chiral limit. The remaining part of the $\frac{1}{2}TrN^2$ term in momentum space is

$$S_{\pi W} = \int \bar{d}^4 p \pi^I(p) W^I_\mu(-p) \times \int \bar{d}^4 q\ tr\left\{ i\gamma_5 \tau^I B(q^2) G(q - \tfrac{1}{2}p) i\frac{g'}{2}\tfrac{1}{2}\tau^J \frac{1}{i}\partial_\mu(\gamma_5 i \not{q} A(q^2)) G(q + \tfrac{1}{2}p)\right\}. \quad (53)$$

Comparison with the bare vertex result (30) indicates that $\gamma_\mu\gamma_5$ has been replaced with $\partial_\mu(\not{q}A)\gamma_5$. This supplies the missing factor of approximately 2 and yields exactly the result (35) at lowest order in p_μ expected from chiral symmetry. Contributions to $S_{\pi W}$ from higher orders in p_μ will be discussed in the next section.

3. $\pi\pi\gamma$ and $\pi\gamma\gamma$

The only part of S contributing to the $\pi\pi\gamma$ interaction comes from the $-\frac{1}{3}TrN^3$ term. As anticipated the effective vertex becomes $ieQ\partial_\mu G^{-1}$ and an integral charge results, which, in contrast to the πW coupling does not depend on NG result $\Gamma_\pi = B$. This is to be expected since the electric charge of the pion is independent of its NG status, whereas the interaction $\partial_\mu \pi^I W^I$ is specific to the non-linear realization of chiral (and hence EW) symmetry implicit in (for example) the gauged σ-model action $tr \int D_\mu U (D_\mu U)^\dagger$.

Calculation of the anomalous $\pi\gamma\gamma$ interaction with the Wilson line method is very complex. We speculate that it also assumes the chiral value.

IV. APPLICATION TO F_K/F_π

In the chiral $SU(3)$ limit $\mathcal{M}_K = \mathcal{M}_\pi = 0$ and $F_K = F_\pi$. The experimental result is $F_K/F_\pi = 1.25$ and in what follows we analyse the GCM predictions using where practicable both the bare vertex and Wilson line methods.

Since Cabibbo angle θ_C dependence is factored out of the definition of F_π, it suffices to examine the behaviour of F_π as the d-quark mass increases to the s-quark mass in order to predict F_K/F_π. A non-zero quark mass affects F_P (where P is the pseudoscalar) in two ways: through direct dependence on the current quark mass and indirectly through being measured on the pseudoscalar mass shell $p^2 = -\mathcal{M}^2$. i.e.

$$F_P(\hat{m}, p^2) = \sum_{i=0}^{\infty} F_P^{(i)}(\hat{m})(p^2)^i \tag{54}$$

where $\hat{m}$ is the average quark mass $(m_u + m)/2$. We define an analogous expansion for the field normalization f_P. In order to calculate the $f_P^{(i)}(m)$ we assume the values

$$m_u = m_d = 10 \text{ Mev} \quad m_s = 100 \text{ MeV} \tag{55}$$

and adjust the value of $f_P^{(0)}(\hat{m})$ so as to produce the experimental value of $\mathcal{M}_k$. We cannot use the PCAC formula (20) as a result of the logarithmic divergence which infects the ladder approximation value of $\langle\bar{q}q\rangle$ [9,29]. This behaviour can be regularized by modifying the asymptotic high-p^2 behaviour of $B(p^2)$ or equivalently of $\alpha(p^2)$, but this introduces a further arbitrary parameter and does not serve to fix the current masses. The values we use are representative of those found in an investigation of the *non*-NG sector in the GCM [14,15], which is not sensitive to the very-high p^2 form of the structure functions. Performing a Taylor series about $p_\mu = 0$ in (33) yields

$$\begin{aligned} f_p^2(0, p^2) &= [0.496 - 0.407p^2 + 0.473p^4 + \mathcal{O}(p^6)] \times 10^{-2} \text{ GeV}^2 \\ f_p^2(\hat{m}_{su}, p^2) &= [0.537 - 0.418p^2 + 0.393p^4 + \mathcal{O}(p^6)] \times 10^{-2} \text{ Gev}^2 \end{aligned} \tag{56}$$

and therefore for the field normalization

$$\frac{f_K}{f_\pi} \approx \frac{f_p(\hat{m}_{su}, -\mathcal{M}_K^2)}{f_p(0,0)} = 1.15 \tag{57}$$

In the bare vertex method, expansion of the Fig. 8 contributions gives

$$\begin{aligned} I_{PW}(0, p^2) &= [0.241 - 0.381p^2 + 0.51p^4 - 0.18p^6 + \mathcal{O}(p^8)] \times 10^{-2} \text{ GeV}^2 \\ I_{PW}(\hat{m}_{su}, p^2) &= [0.233 - 0.333p^2 + 0.437p^4 - 0.15p^6 + \mathcal{O}(p^8)] \times 10^{-2} \text{ Gev}^2 \end{aligned} \tag{58}$$

and

$$\left[\frac{F_K}{F_\pi}\right]_{bare\ vertex} \approx \frac{I_{PW}(\hat{m}_{su}, -\mathcal{M}_K^2)}{I_{PW}(0,0)} \times \frac{f_\pi}{f_K} = 1.20 \qquad (59)$$

In the Wilson line method, expansion of the terms in Fig. 8 to order (p^2) and using a straight line yields

$$I_{PW}^{Wilson}(0,p^2) = [0.496 + (-0.767 - 0.461 + 0.095)p^2 + \mathcal{O}(p^4)] \times 10^{-2}\ \text{GeV}^2$$
$$I_{PW}^{Wilson}(\hat{m}_{su},p^2) = [0.476 + (-0.662 - 0.391 + 0.098)p^2 + \mathcal{O}(p^4)] \times 10^{-2}\ \text{Gev}^2 \qquad (60)$$

and hence to order (p^2)

$$I_{PW}^{Wilson}(\hat{m}_{su}, -\mathcal{M}_K^2) = 0.709\ . \qquad (61)$$

Therefore

$$\left[\frac{F_K}{F_\pi}\right]_{Wilson} \approx 1.24 + \Delta\ . \qquad (62)$$

Δ is in principle calculable but of a rather co..plicated form. On the basis of the behaviour of the higher order bare vertex contributions, we estimate $\Delta \approx 0.06$.

Both the Wilson and bare vertex estimates are acceptably close to the experimental value of 1.25. Use of the EW gauge-invariant Wilson line differs from the bare vertex result by about 10 per cent. If the function $A(p^2)$ were more steeply varying, the results would differ by a greater amount.

A prediction of this analysis is that at $p^2 = 0$, $F_K/F_\pi \approx 1.03$. The p^2 dependence may be tested in K_{l3} decays.

V. APPLICATION TO $\pi^\pm$ CHARGE RADIUS

On the basis of vector dominance [26] one would expect the k^2 dependence of diagrams such as Fig. 6(b) to be much too small to account for the experimentally observed pion charge radius, since the tree level contribution of Fig. 9 would be expected to dominate. In the Wilson line method, the VA coupling (where V is a vector meson and A is the photon) is gauge-invariant and contributes only to the pion charge radius and not at all to the charge - this is the result of a cancellation similar to those already discussed which produces a zero coupling at $k_\mu = 0$. In the bare vertex method, the VA coupling contributes to both charge and charge radius with a non-gauge invariant part which survives at $k_\mu = 0$ of the form $\int V_\mu A_\mu$. Calculation of the vector meson couplings, which would enable a computation of the vector meson contribution, is beyond the scope of this paper, requiring accurate knowledge of the ρ_μ and ω_μ structure functions on and off shell.

For reasons of computational ease we look at the k^2 dependence of the bare vertex form of Fig. 6(b) to get a rough estimate of the contribution of the 'direct' diagram.

We find that the direct contribution to the charge radius is 1.2 GeV^{-2}, compared with the experimental charge radius

$$\langle r^2_{\pi^\pm} \rangle \approx \frac{6}{M^2_\rho} \approx 10\ \mathrm{GeV}^{-2}\ . \tag{63}$$

As expected the direct contribution is very small, consistent with vector dominance.

Ebert and Volkov [17] have shown how vector dominance may be derived from a Namb-Jona-Lasinio lagrangian using (local) bosonization. The EW gauge fields are completely removed from the $Tr\ Ln$ by absorbing them into the definition of the (composite,local) vector and axial vector mesons, reappearing outside the $Tr\ ln$ as interaction terms with these fields of the familiar vector dominance form $\rho_\mu A_\mu$. (not to be confused with the spurious contibution of this form in the bare vertex method above). Hence by a shift of the composite fields the EW fields are shown to interact effectively with all hadrons only via the vector and axial vector mesons. That such a result is achieved depends on the vector and axial vector mesons having the same (minimal) γ_μ coupling with the effective quarks as the EW gauge fields. In the more detailed GCM, and assuming that a gauge invariant scheme such as the Wilson line method should be used, the EW gauge fields cannot in general be removed from the $Tr\ ln$ in (48) by a simple shift of the $\rho, \omega \ldots$ components of $M^\theta_m \mathcal{B}^\theta(x,y)$: the structure functions at low transfer momentum k would have to coincide with those of the EW fields. For the case of electromagnetism the vector meson structure function (a solution of the homogenous Bethe-Salpeter equation) is very likely not of the photon-vertex form $\partial_\mu G^{-1}(q)$, where q is the effective quark momentum. One would expect the required shift in $\mathcal{B}$ to involve other resonances which would then interact directly with photons A_μ along with the ρ_μ and ω_μ and their radial excitations through the second term of (48).

VI. CONCLUSION

Any QCD-inspired study of the low-energy behaviour of hadrons must involve effective quark propagators with momentum-dependent propogators, which complicates the gauge-invariant calculation of EW properties of hadrons. In the context of the Global Color Model, which can be derived as a truncation of QCD, we have discussed how such predictions can be extracted, and we have introduced a modified bosonization involving Wilson lines which maintains chiral and electromagnetic current conservation at tree level. A computation of F_K/F_π in the GCM accounts satisfactorily for the experimental value of 1.25, and a GCM prediction is that at $p^2 = 0$, F_K/F_π is very close to the chiral $SU(3)$ value of 1. Analysis of the $\pi^\pm$ charge radius gives qualitative support for vector dominance; however a 'proof' of vector dominance previously given for an NJL model does not survive the additional complications of the

GCM. A convincing account of the role played by vector dominance would need to involve knowledge of the off-shell behaviour of vector meson structure functions and the contribution of scalar and other mesons.

VII. ACKNOWLEDGEMENTS

The authors wish to thank J. Praschifka, R.T. Cahill, and G. Adam for useful discussions. C.B. wishes to thank the staff of the Research School of Physical Sciences at the Australian National University for their kind hospitality during part of this period. C.B. also acknowledges the financial support of an Australian Postgraduate Research Award.

[1]For a recent review see R. W. Haymaker, Louisiana State University Preprint LSU-HE-108-1990.

[2]R. W. Haymaker and J. Perez-Mercader, Phys. Rev. D**27**, 1353 (1983); R. W. Haymaker, T. Matsuki and F. Cooper, Phys. Rev. D**35**, 2567 (1987).

[3]D. W. McKay and H. J. Munczek, Phys. Rev. D**40**, 4151 (1989).

[4]D. W. McKay, H. J. Munczek and B. L. Young, Phys. Rev. D**37**, 195 (1988).

[5]V. Sh. Gogokhia, Gy. Kluge and B. A. Magradze, Phys. Lett. **244B**, 68 (1990).

[6]R. T. Cahill and C. D. Roberts, Phys. Rev. D.**32**, 2419 (1985).

[7]C. D. Roberts and R. T. Cahill, Aust. J. Phys. **40**, 499 (1987).

[8]J. Praschifka, C. D. Roberts and R. T. Cahill, Phys. Rev. D**36**, 209 (1987).

[9]R.T. Cahill, C. D. Roberts and J. Praschifka, Phys. Rev. D**36**, 2804 (1987).

[10]J. Praschifka, C. D. Roberts and R. T. Cahill, Int. J. Mod. Phys. A**2**, 1797 (1987).

[11]C. D. Roberts, R. T. Cahill and J. Praschifka, Int. J. Mod. Phys. A**4**, 719 (1989).

[12]J. Praschifka, R. T. Cahill and C. D. Roberts, Mod. Phys. Lett. A**3**, 1595 (1988).

[13]R. T. Cahill, J. Praschifka and C. J. Burden, Aust. J. Phys. **42**, 161 (1989); R. T. Cahill, Aust. J. Phys. **42**, 171 (1989); R. T. Cahill in *Workshop on Diquarks*, Villa Gualino, Torin, Italy. Oct. 24-26 1988, edited by Mauro Anselmino and Enrico Predazzi (World Scientific).

[14]C. D. Roberts, R.T. Cahill, and J. Praschifka, Ann. Phys. **188**, 20 (1988).

[15]R. T. Cahill, C. D. Roberts and J. Praschifka, Aust. J. Phys. **42**, 129 (1989).

[16]C. J. Burden, R. T. Cahill and J. Praschifka, Aust. J. Phys. **42**, 147 (1989).

[17]D. Ebert and M. Volkov, Z. Phys. C**16**, 205 (1983); Ann. Phys. **157**, 282 (1984).

[18]D. Ebert and H. Reinhardt, Nucl. Phys. B**271**, 188 (1988).

[19]D. Kahana and U. Vogl, Phys. Lett. **244B**, 10 (1990).

[20]S. Theberge, A. W. Thomas and G. A. Miller, Phys. Rev. D**22**, 2838 (1980); A. W.

Thomas, S. Theberge and G. A. Miller, Phys. Rev. D**24**, 216 (1981); G. E. Brown and M. Rho, Phys. Lett. **82B**, 177 (1979); A. W. Thomas, Adv. Nucl. Phys. **13**, 1 (1984).

[21]J. Praschifka, Ph.D. Thesis (Flinders University of South Australia 1988).

[22]H. Hamber and G. Parisi, Phys. Rev. Lett. **47**, 1792 (1981).

[23]M. Lutz and J. Praschifka, Regensburg Preprint TPR-90-47.

[24]D. Atkinson and D. W. E. Blatt, Nucl. Phys. B**151**, 342 (1979).

[25]T. Goldman and R. W. Haymaker, Phys. Rev. D**24**, 724 (1981).

[26]B. Bagchi, A. Lahiri and S. Niyogi, Phys. Rev. D**39**, 3384 (1989).

[27]R. P. Feynman, *Photon-Hadron Interactions* (W. A. Benjamin 1972).

[28]J. Wess and B. Zumino, Phys. Lett. **37B**, 96 (1971).

[29]R. T. Cahill, private communication.

FIG. 1. Classes of diagrams in a perturbation expansion of QCD. The grey circles with n gluons emerging are full (reducible) n-point functions for QCD without quarks.

FIG. 2. Plot of the numerical solution of the quark propagator A and B functions.

FIG. 3. Terms contributing at tree level to the generation of meson kinetic and mass terms in position space. The grey circles are the 'ladder' approximation structure functions.

FIG. 4. One-loop corrections to meson propagation

FIG. 5. One-loop tadpole signalling a vacuum shift

FIG. 6. Terms in the expansion of the $TrLn$ in momentum space for the bare vertex method for the processes (a) $\pi^{\pm}$ decay constant F_π; (b) $\pi^{\pm}$ charge; (c) anomalous $\pi^0 \to \gamma\gamma$ decay

FIG. 7. Routing of Wilson lines (a) before and (b) after the Fierz transformation

FIG. 8. The terms contributinf to F_π in the Wilson line method. The striped ovals denote Wilson-line dependent vertices.

FIG. 9. Tree level vector meson contribution to the charge radius

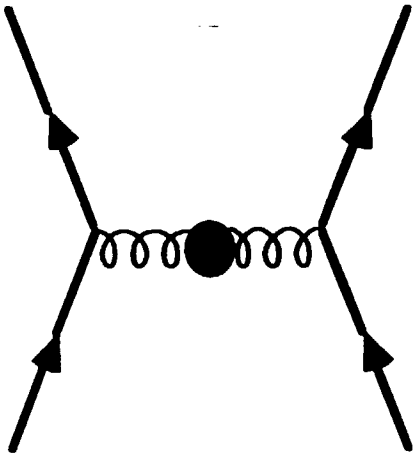

(a)

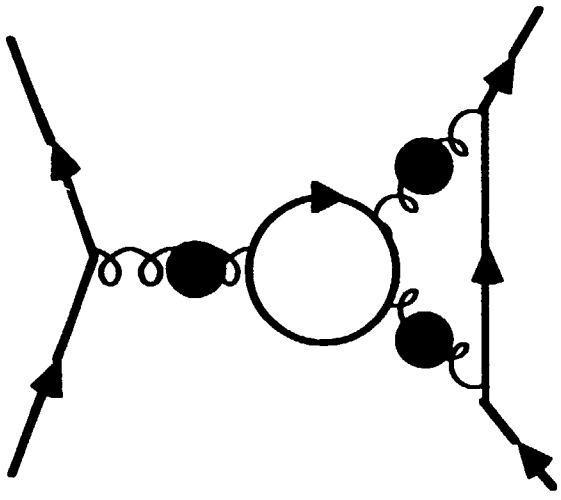

(b)

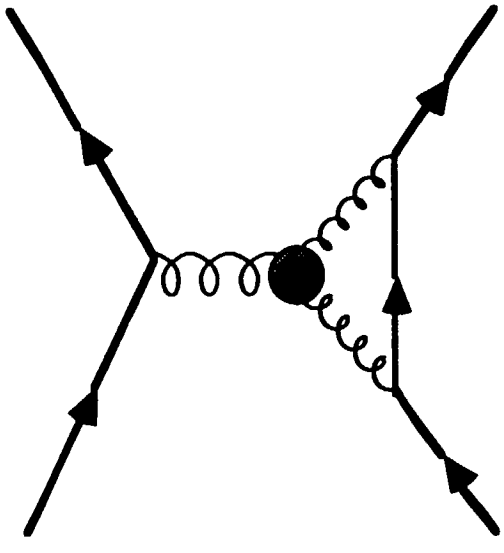

(c)

Figure 1

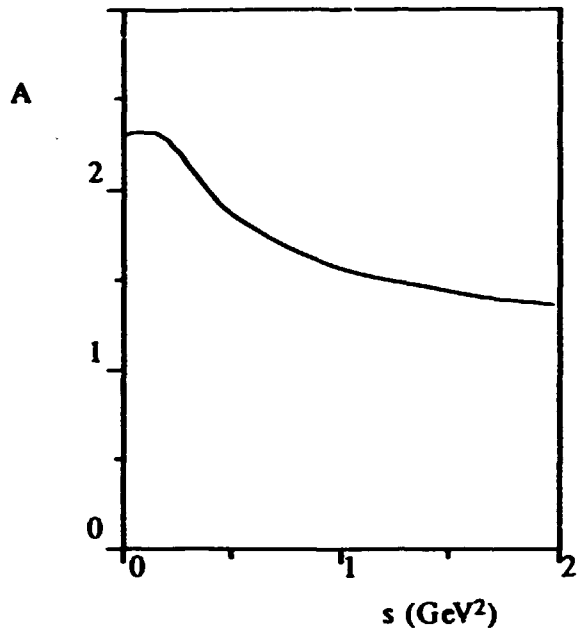

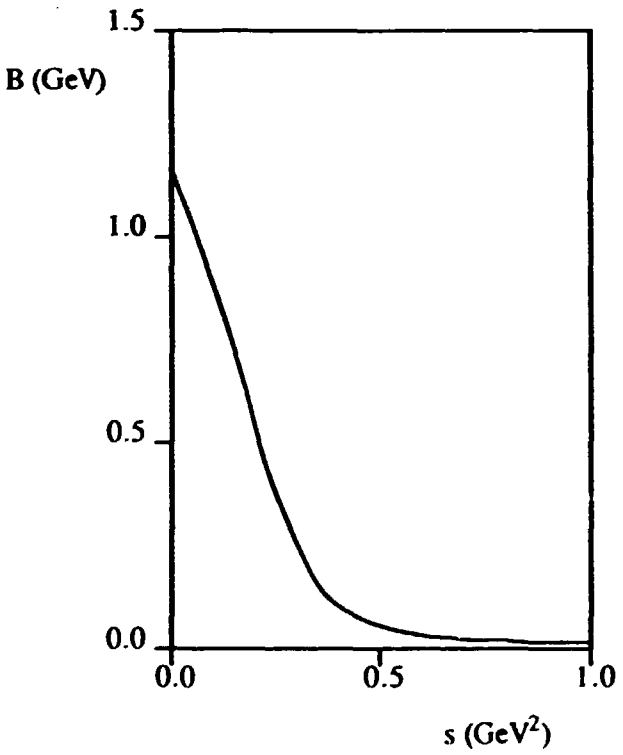

Figure 2

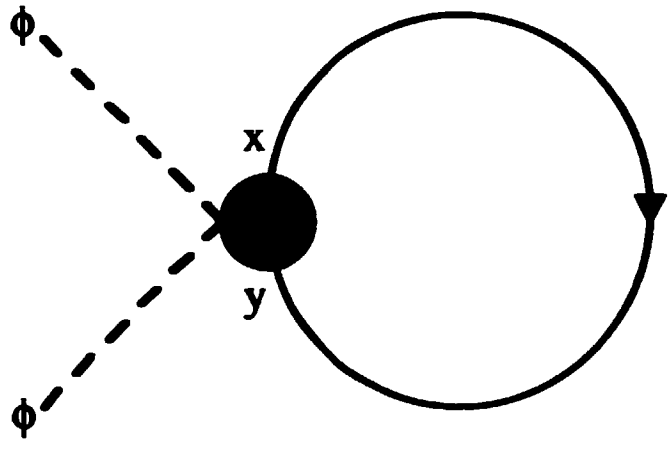

(a)

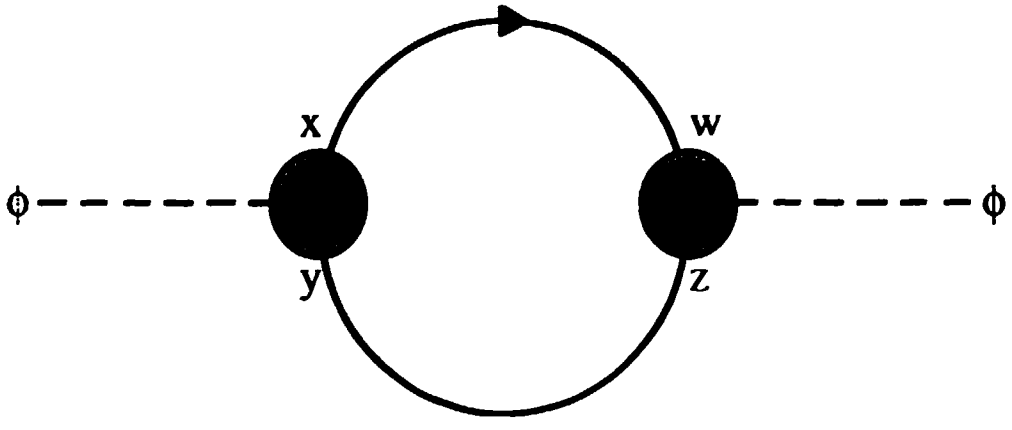

(b)

Figure 3

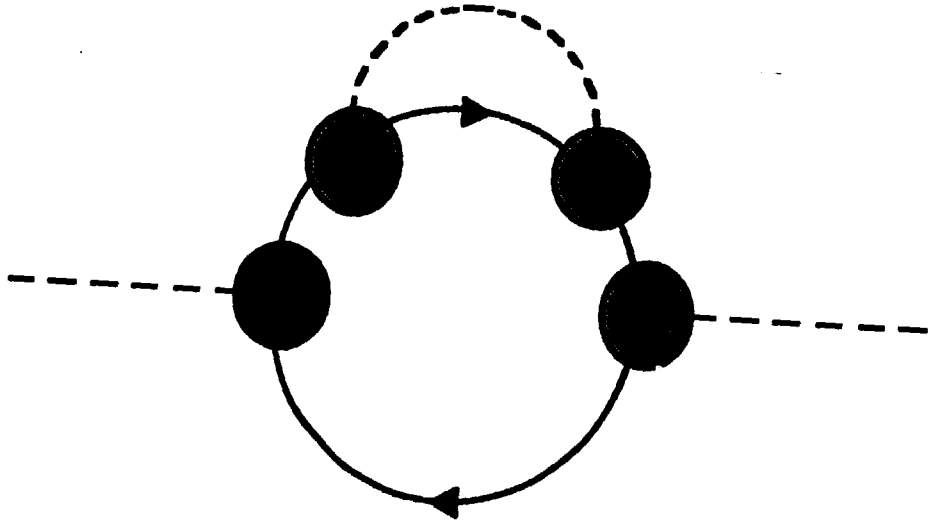

(a)

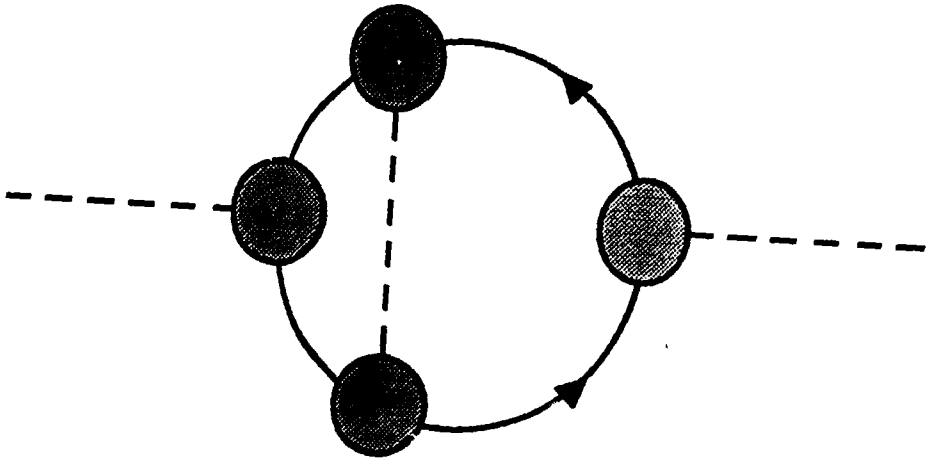

(b)

Figure 4

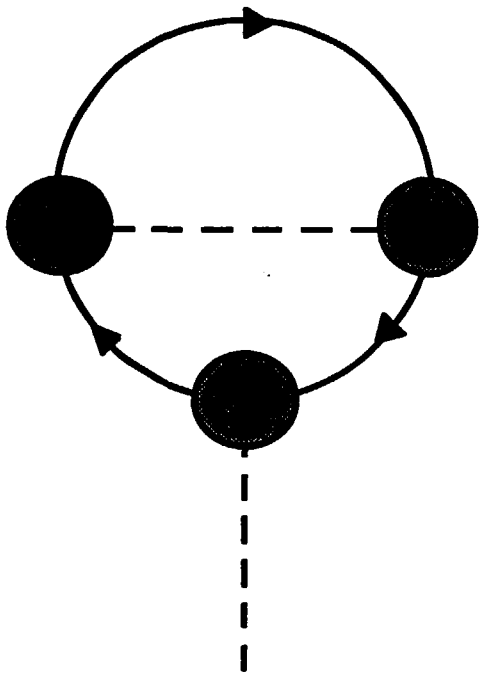

Figure 5

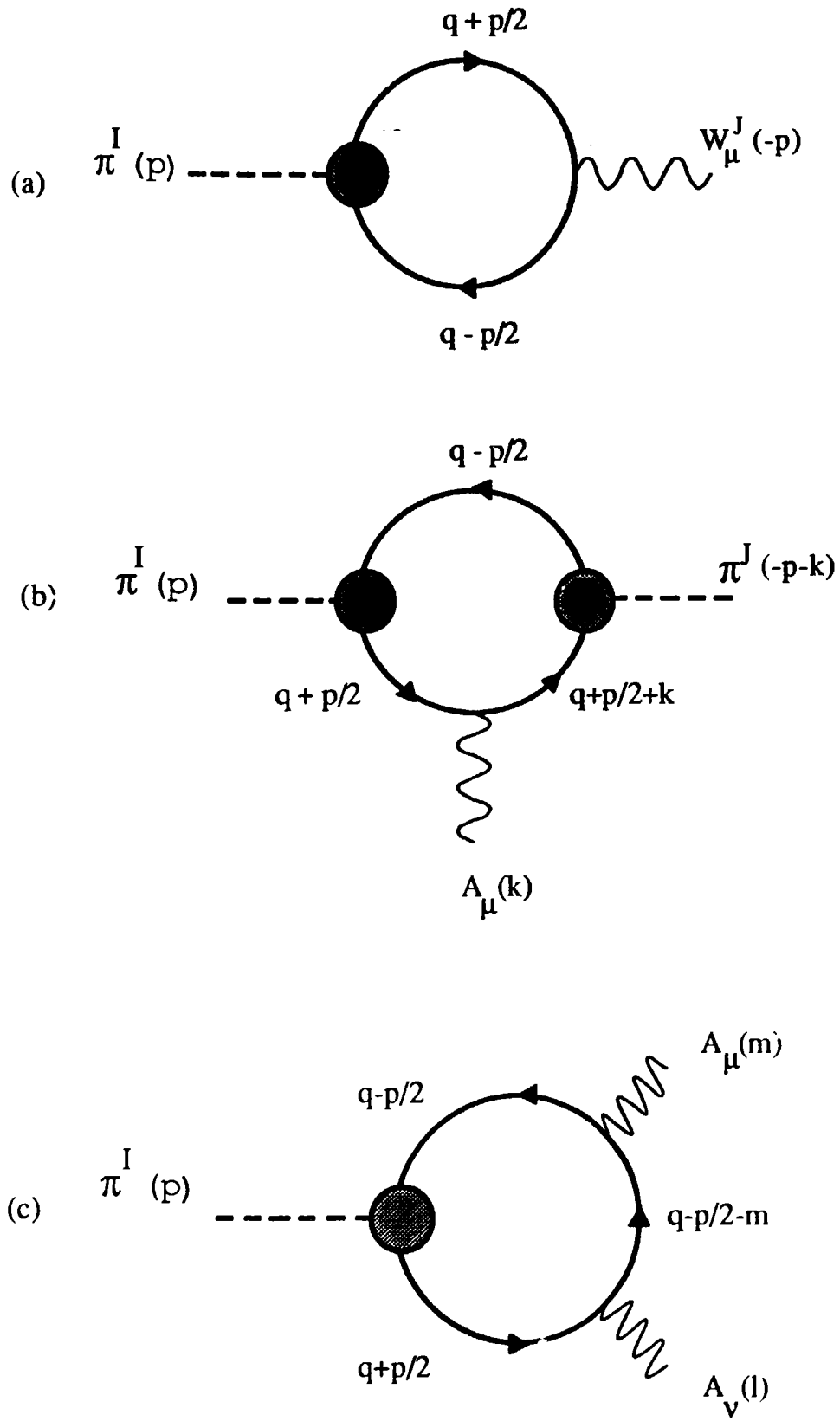
(a)
π^I (p)
q + p/2
q - p/2
W_μ^J (-p)
(b)
π^I (p)
q - p/2
q + p/2
q+p/2+k
π^J (-p-k)
A_μ(k)
(c)
π^I (p)
q-p/2
q-p/2-m
q+p/2
A_μ(m)
A_ν(l)

Figure 6

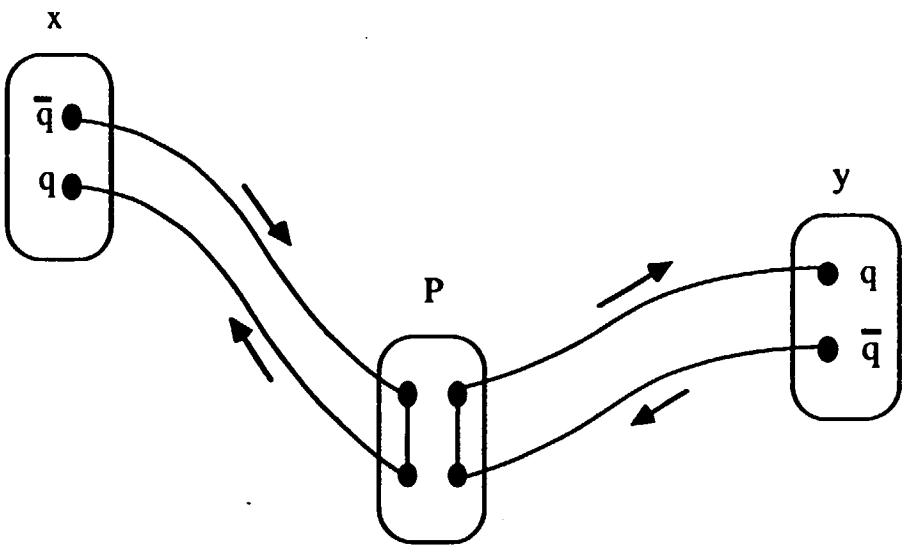

(a)

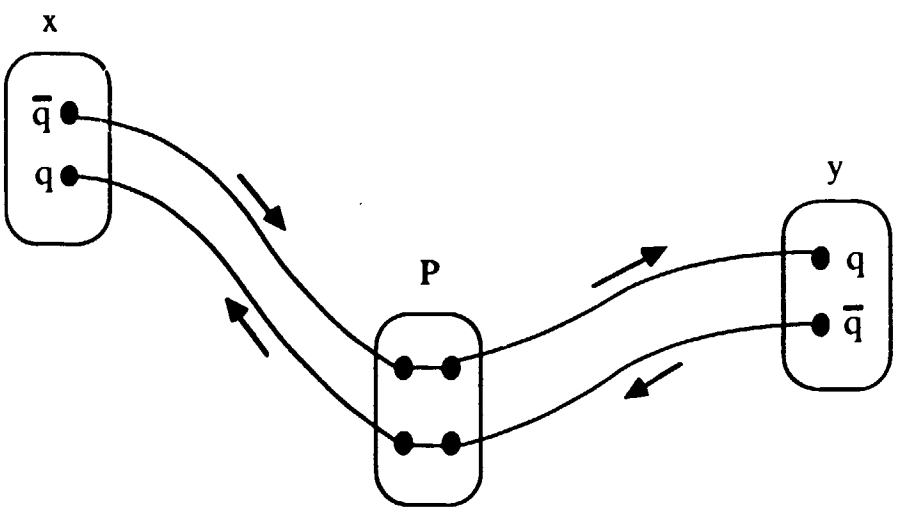

(b)

Figure 7

(a)

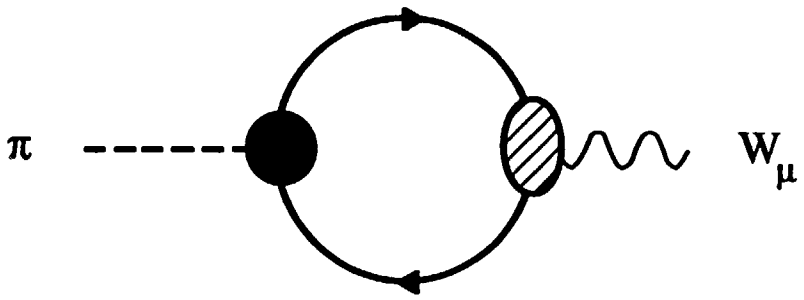

(b)

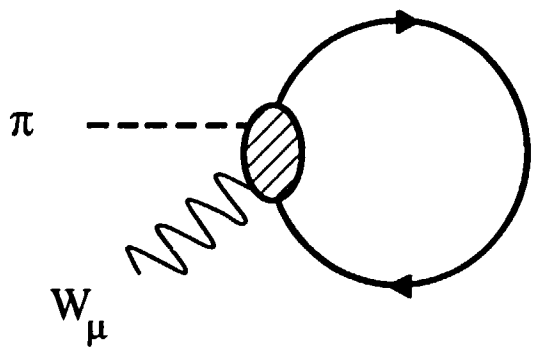

Figure 8

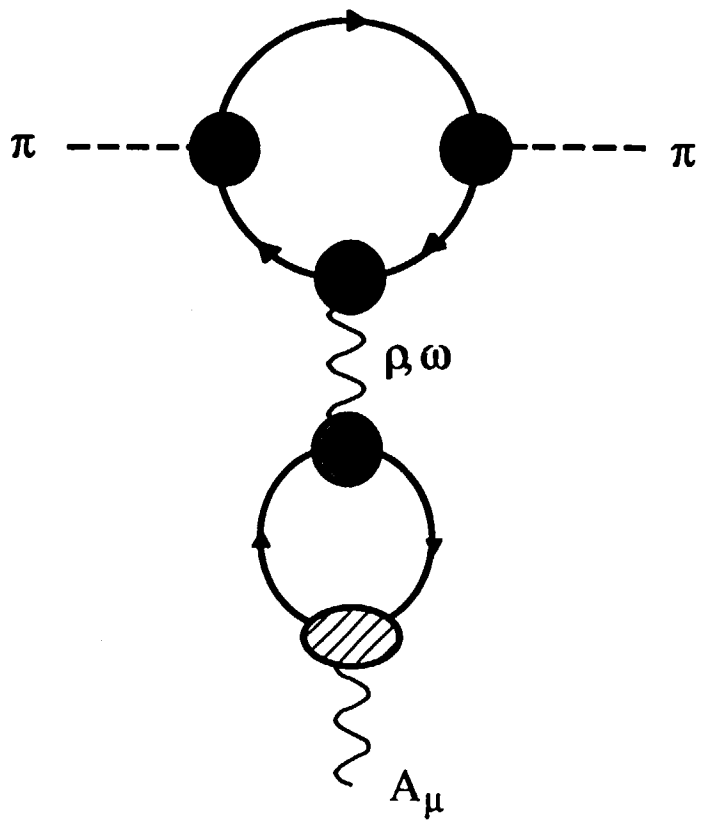

Figure 9